

**Revisiting prompt emission calculations for
 $^{252}\text{Cf}(\text{SF})$ with focus on post-neutron fragment
distributions and different correlations**

Anabella Tudora

University of Bucharest, Faculty of Physics

WONDER-2023

Both models **PbP** and **DSE** developed during the time at the University of Bucharest are based on a **deterministic treatment of prompt emission and a deterministic construction** of the fragmentation and TKE ranges, leading to a **large number of initial configurations {A, Z, TKE}** for which the calculations are done.

The deterministic treatment allows to take into account also fragmentations which appear with a very low probability, this being an advantage especially in the case of independent FPY calculations.

This deterministic construction of the fragmentation range consists of:

- a large range of pre-neutron (initial) fragment masses **A**: going from symmetric fission up to a very asymmetric split (with a step of 1 mass unit)
- 5 charge numbers **Z** per **A** are taken, as the nearest integers above or below the most probable charge $Z_p(A) = Z_{UCD}(A) + \Delta Z(A)$.

The Isobaric charge distributions $p(Z,A)$ are Gaussian functions centered on $Z_p(A)$ with ΔZ and rms as a function of **A** ($\Delta Z(A)$ and rms(A) being usually provided by the Z_p model of Wahl)

- for each fragmentation (fragment pair) a large TKE range is considered

²⁵²Cf(SF) by taking $A = 77 - 175$, with 5 Z / A , $TKE = 130 - 230$ MeV (step 2 MeV) and excluding un-physical cases (e.g. $Q-TKE < 0$) → **the number of (A,Z,TKE) configurations is of about 17000 – 18000**

PbP – based on a **global treatment of prompt emission** so that its primary results consists of matrices of different quantities $q(A,Z,TKE)$ which are an average over the emission sequences

DSE – based on a **detailed treatment sequence by sequence**, so that its primary results consists of matrices corresponding to each emission sequence $q_k(A,Z,TKE)$ with $k = 1$ to $n(A,Z,TKE)$

In the DSE model the post-neutron fragment, i.e. the last residual fragment (corresponding to each initial configuration) is well determined, its mass number **$A_p(A,Z,TKE) = A - n(A,Z,TKE)$** being **an integer**. So that this approach is appropriate for the calculation of independent FPY ($Y(Z,A_p)$, $Y(A_p)$), different distributions of KE_p , and different correlations between quantities of the pre- and post-neutron fragments etc. Consequently it is used in this investigation.

➤ Any prompt emission treatment is **strongly influenced by the energy partition in fission**, which is known as **“TXE partition”**, even if the energy sharing takes place at scission or even before scission (in some models).

➤ The single distributions related to prompt emission ($\nu(A)$, $\nu(\text{TKE})$, $\langle \varepsilon \rangle(A)$, $\langle \varepsilon \rangle(\text{TKE})$, $E_\gamma(A)$, $E_\gamma(\text{TKE})$, $M_\gamma(A)$, $M_\gamma(\text{TKE})$ etc.) and the total average values of prompt emission quantities (e.g. $\langle \nu \rangle$, $\langle E_\gamma \rangle$, prompt neutron and γ -ray spectra) as well as well as independent FPY, KE_p distributions etc.

depend on the distribution $Y(A, \text{TKE})$ of pre-neutron fragments (such $Y(A, \text{TKE})$ being input data in a great part of prompt emission model codes).

The **influence of both the $Y(A, \text{TKE})$ distribution of pre-neutron fragments and the TXE partition** on prompt emission results and on post-neutron fragment distributions and different correlations **is investigated** in this work as follows :

I. Three pre-neutron fragment distributions $Y(A, \text{TKE})$ of $^{252}\text{Cf}(\text{SF})$ are considered. They were measured at EC-JRC-Geel during the time:

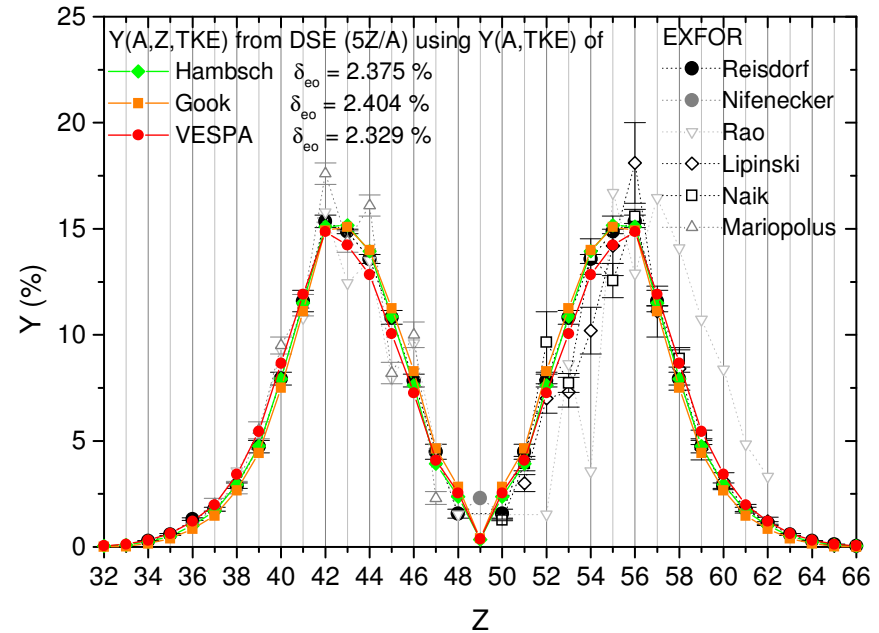
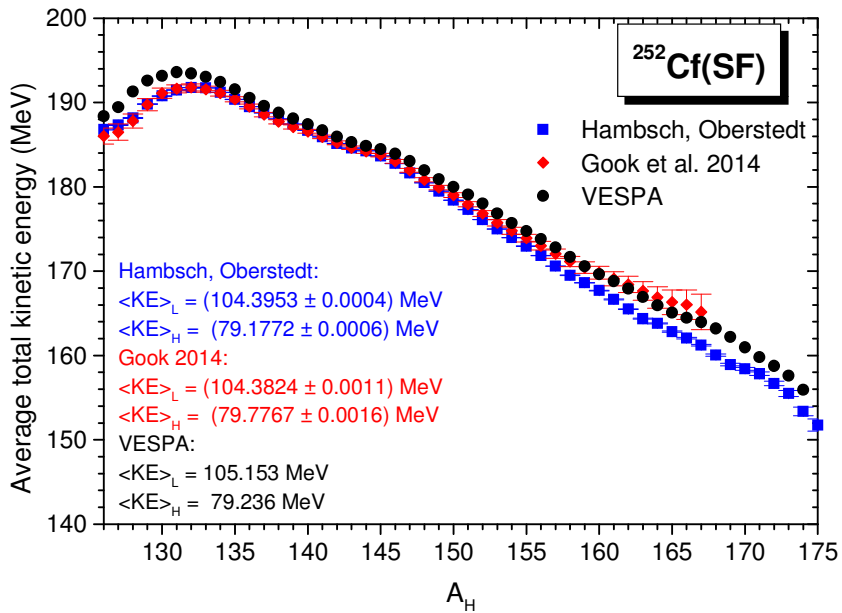
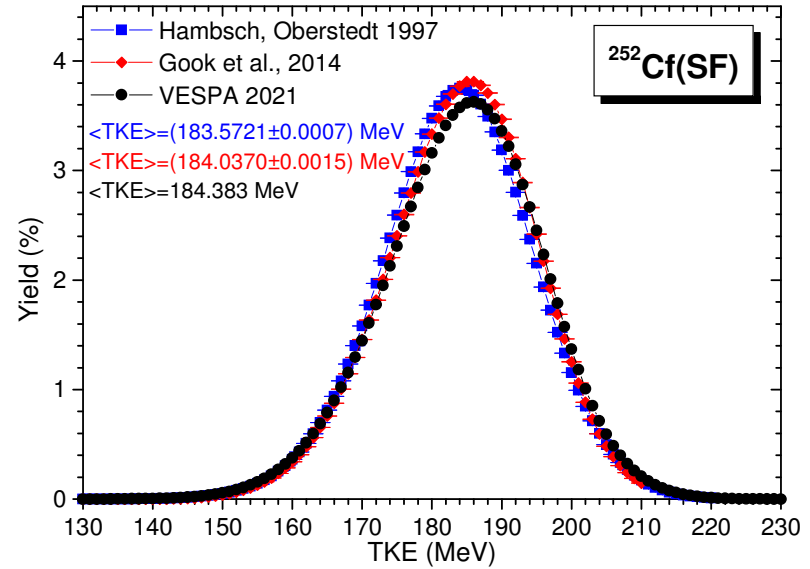
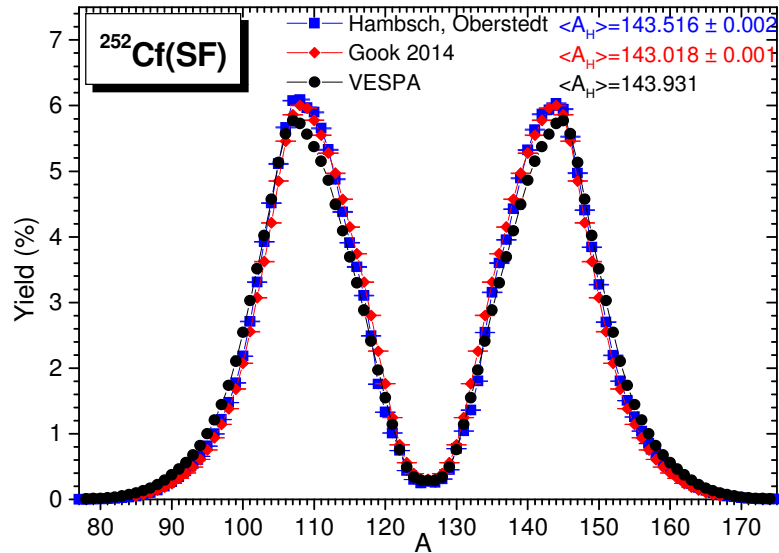
- 1) **Hambsch and Oberstedt, Nucl.Phys.A 617 (1997) 347**
- 2) **Göök et al., Phys.Rev.C 90 (2014) 064611**
- 3) **In the VESPA experiment (Travar et al., Phys.Lett.B 817 (2021) 136293**

These $Y(A, \text{TKE})$ data enter the multiple pre-neutron fragment distribution:

$$Y(A, Z, \text{TKE}) = p(Z, A) Y(A, \text{TKE})$$

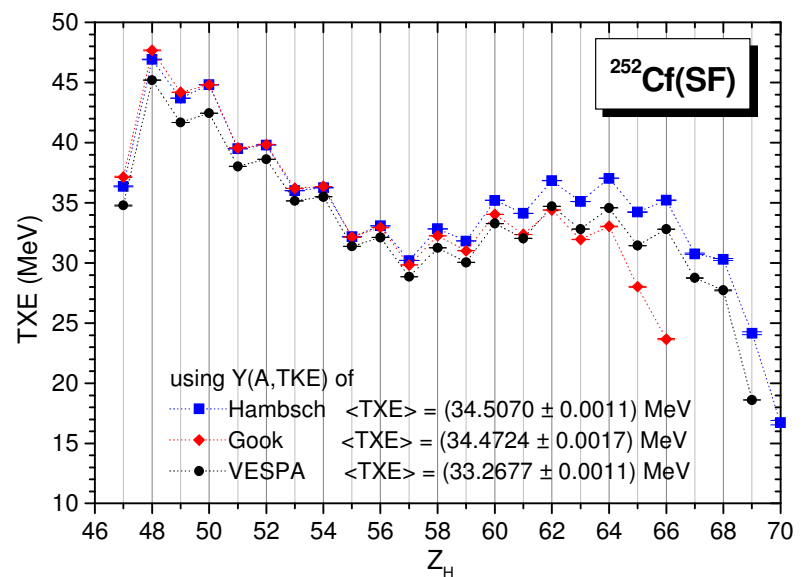
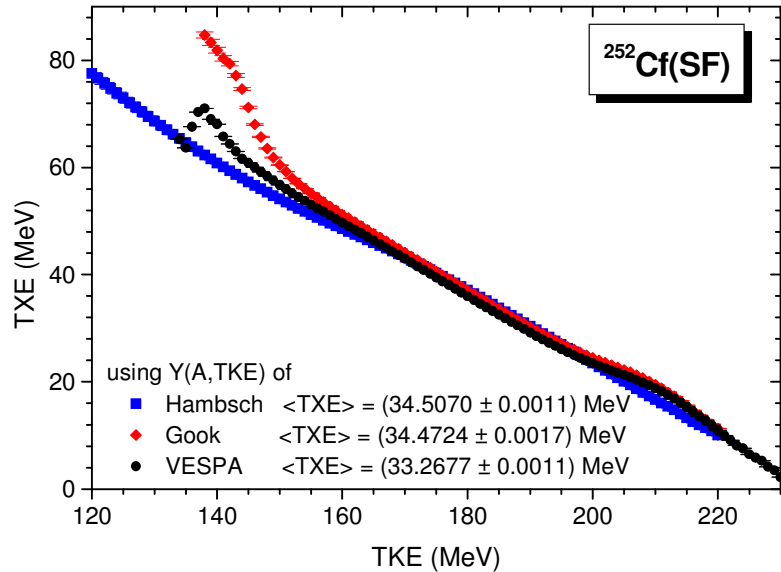
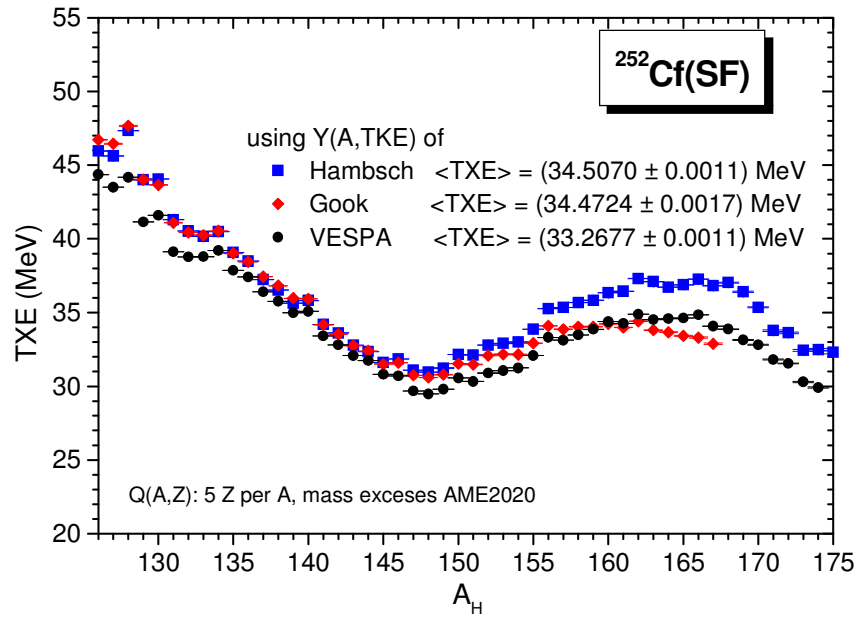
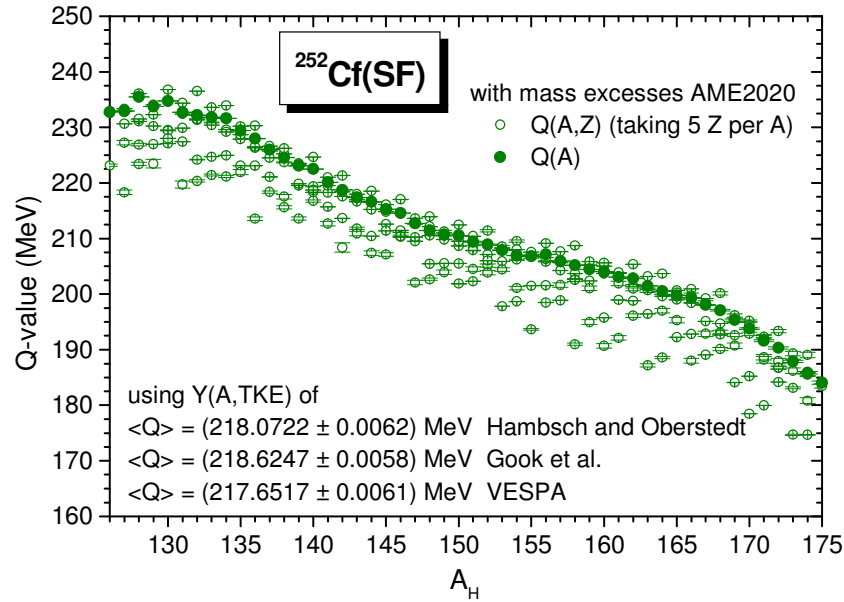
The primary results of DSE (consisting of matrices $q_k(A, Z, \text{TKE})$) are averaged over this $Y(A, Z, \text{TKE})$ distrib. in order to obtain prompt emission results as single distributions, total average values of prompt emission quantities, yields and other distributions of post-neutron fragments

The differences between the three $Y(A, TKE)$ data are better visible in 2D representations: $Y(A)$, $TKE(A)$, $Y(TKE)$, as well as in $Y(Z)$ resulting from $Y(A, Z, TKE)$ based on these $Y(A, TKE)$ data



Before to proceed to the energy partition in fission (TXE partition)

Influence of $Y(A, TKE)$ on quantities characterizing the fragmentation (fragment pair)



II. Methods of energy partition in fission

The TXE partition methods are classified in 2 categories (differing as principle), i.e.

- i) methods based on different physical considerations and assumptions about what is happening at scission, known as methods based on **modeling at scission**
- ii) methods in which the sharing of TXE is done directly at the full acceleration of fragments being based on **different parameterizations**

We have chosen one method of each category:

I. **Our method based on modeling at scission** (developed more than 10 y ago) which is incorporated into the model codes PbP and DSE (e.g. *Tudora et al., Nucl.Phys.A 940 (2015) 242, Eur.Phys.J.A 53 (2017) 159, 54 (2018) 87* etc.)

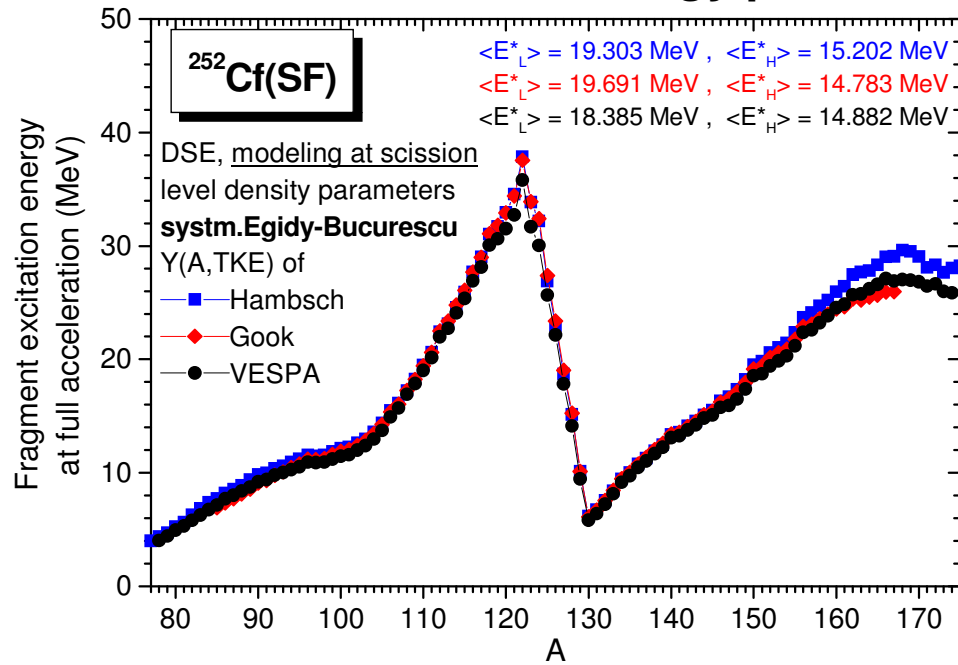
II. The sharing of TXE according to the temperature ratio $R_T = T_L/T_H$ of fully accelerated FF (which is given as input) as following:

- either R_T is taken as a function of A_H , which is fitted to match the experimental data of prompt neutron multiplicity $\nu(A)$ as in the CGMF code
- or R_T is an unique input value (the same for all fragmentations) as in the HF³D code

In the previous studied case $^{235}\text{U}(n_{th},f)$ [*Tudora, Eur.Phys.J.A 58 (2022) 126*] the use of $R_T = 1.2$ (as in the HF³D code) has led to DSE results of prompt emission and independent FPY in very good agreement with the experimental data. Moreover the total average $\langle R_T \rangle$ resulting from our energy partition based on modeling at scission (with different prescriptions for the level dens. parameter) was of about 1.2, too. *This fact can be considered as a simultaneous validation of both methods, our modeling at scission and R_T of HF³D.*

In the case of $^{252}\text{Cf}(SF)$ the use of an unique value of R_T i.e. $\langle R_T \rangle$ of about 1.1 resulting from modeling at scission) does not lead to $\nu(A)$ in agreement with the experimental data. → So that we have used a **parameterization of $R_T(A_H)$** by a few jointed segments which approximates very well the shape of $R_T(A_H)$ obtained from our method based modeling at scission.

Two methods of energy partition in fission used in this investigation



← TXE partition based on our modeling at scission

Consisting of:

- extra-deformation energy: difference between the absolute deformation energy of a fragment at scission and at its full acceleration
- sharing of available excitation energy at scission under the assumptions: statistical equilibrium at scission and fragment level densities in the Fermi-gas regime

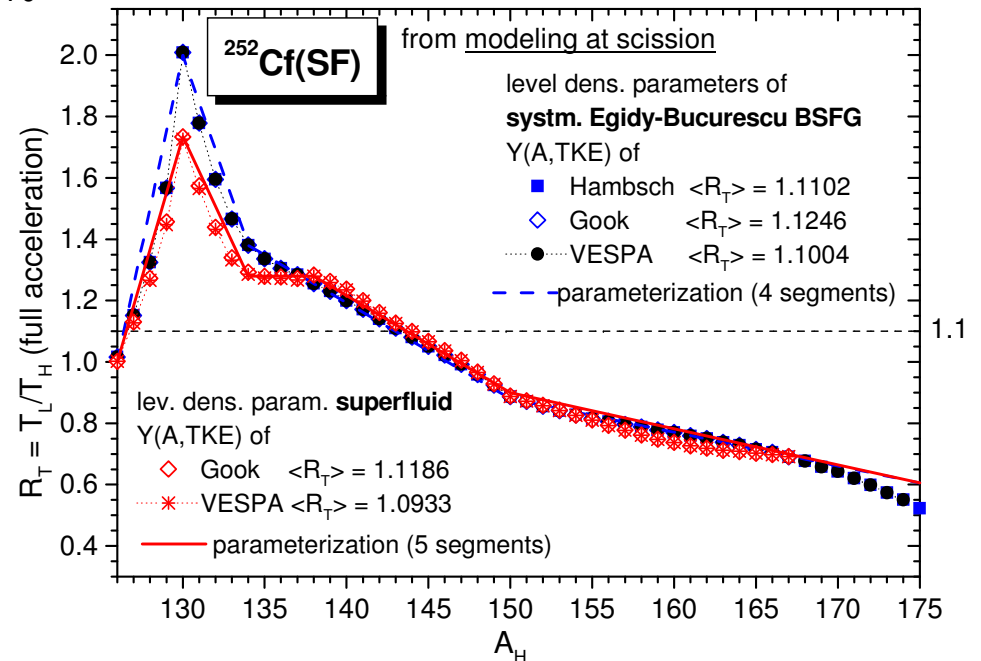
Different prescriptions for the level density parameter can be employed

The sharing of TXE is done according to the $R_T(A_H)$ parameterization by jointed segments

$$R_T = \frac{T_L}{T_H} = \sqrt{\frac{a_H E_L^*}{a_L E_H^*}} \quad \text{obtained from modeling at scission} \rightarrow$$

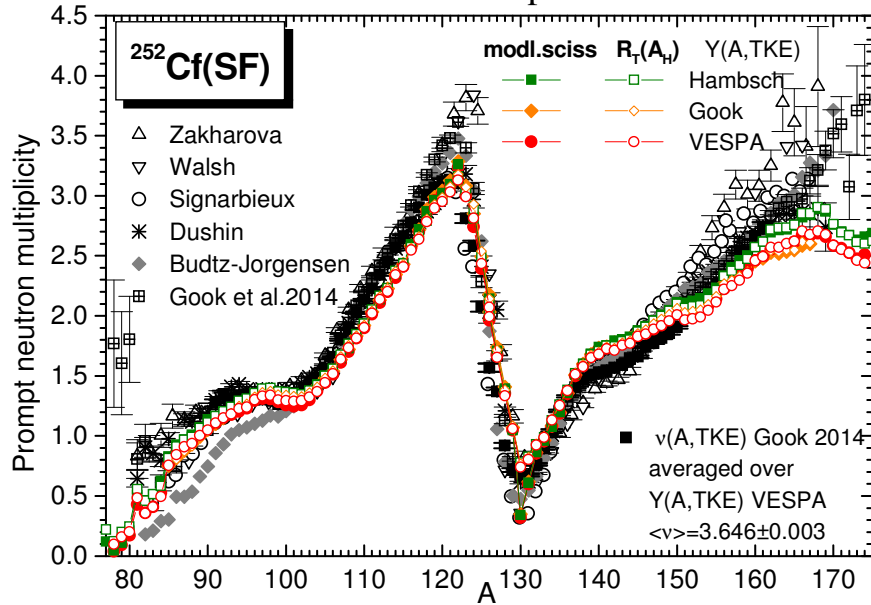
i.e. $E_{L,H}^*$ are those of fully accelerated FF obtained from the energy partition based on modeling at scission with different prescriptions for the level density parameters $a_{L,H}$ at scission and at full acceleration (here the superfluid model and the systematic of Egidy-Bucurescu for BSFG).

The shape of $R_T(A_H)$ is parameterized by a few jointed segments → the continuous red line

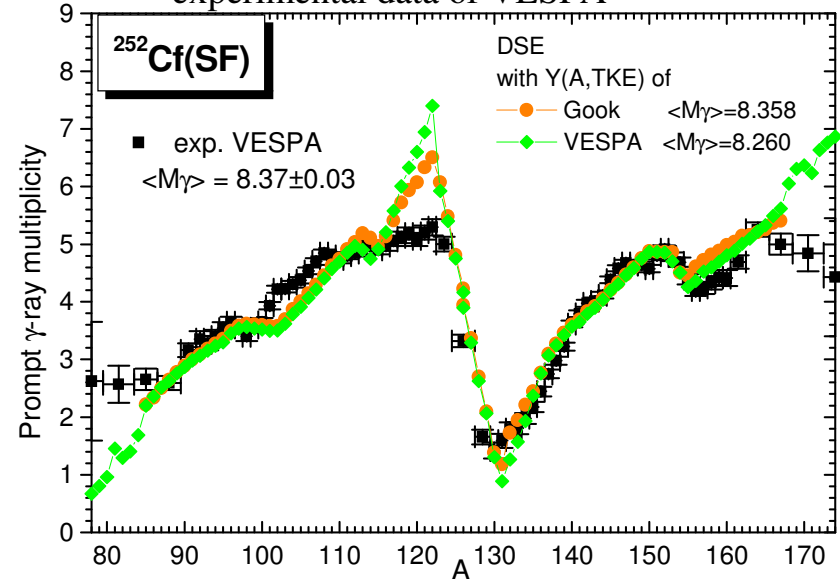


Examples of DSE results of prompt emission quantities

The $\nu(A)$ result plays the most important role in the determination of independent FPY



$M_\gamma(A)$ results compared with the recent experimental data of VESPA



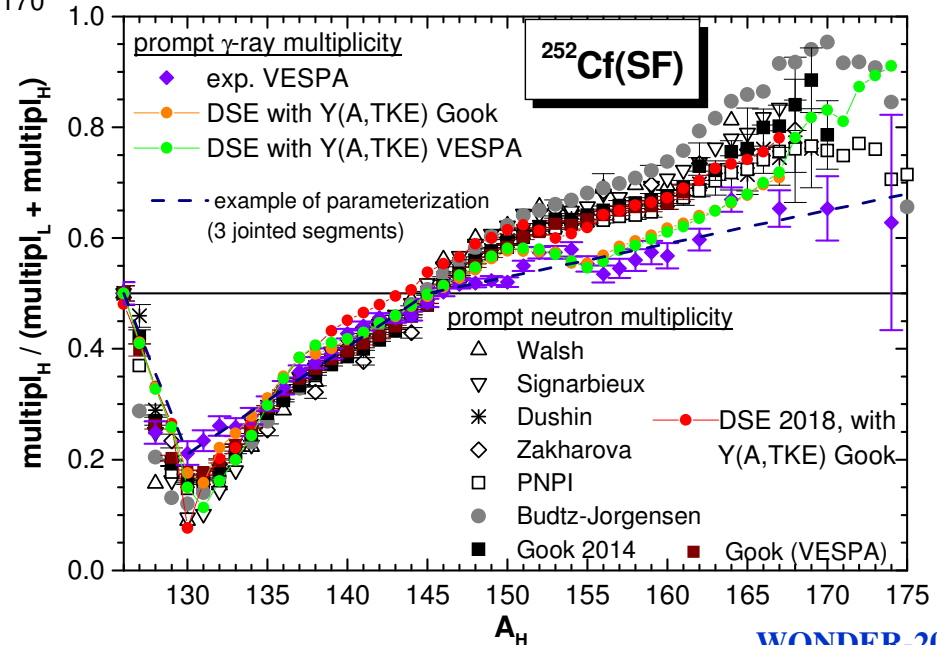
Both multiplicity ratios as a function of A_H
(i.e. the multiplicity of heavy fragment divided to that of fragment pair)

of prompt neutrons $\nu_H/(\nu_L+\nu_H)$

and

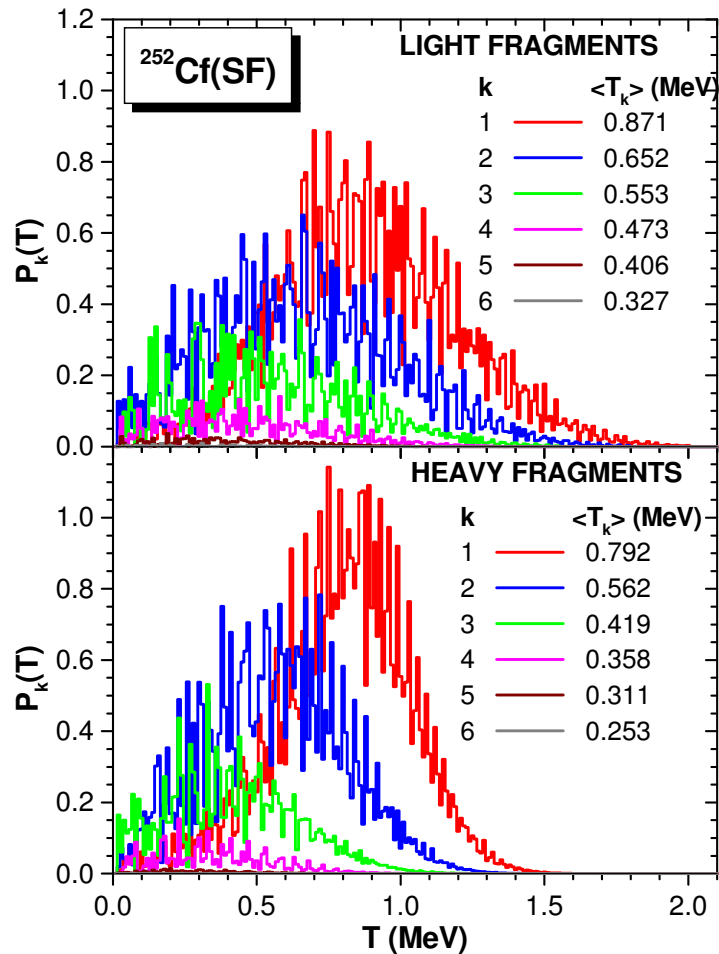
of prompt γ -rays $M_{\gamma_H}/(M_{\gamma_L}+M_{\gamma_H})$

exhibit almost the same behaviour \rightarrow

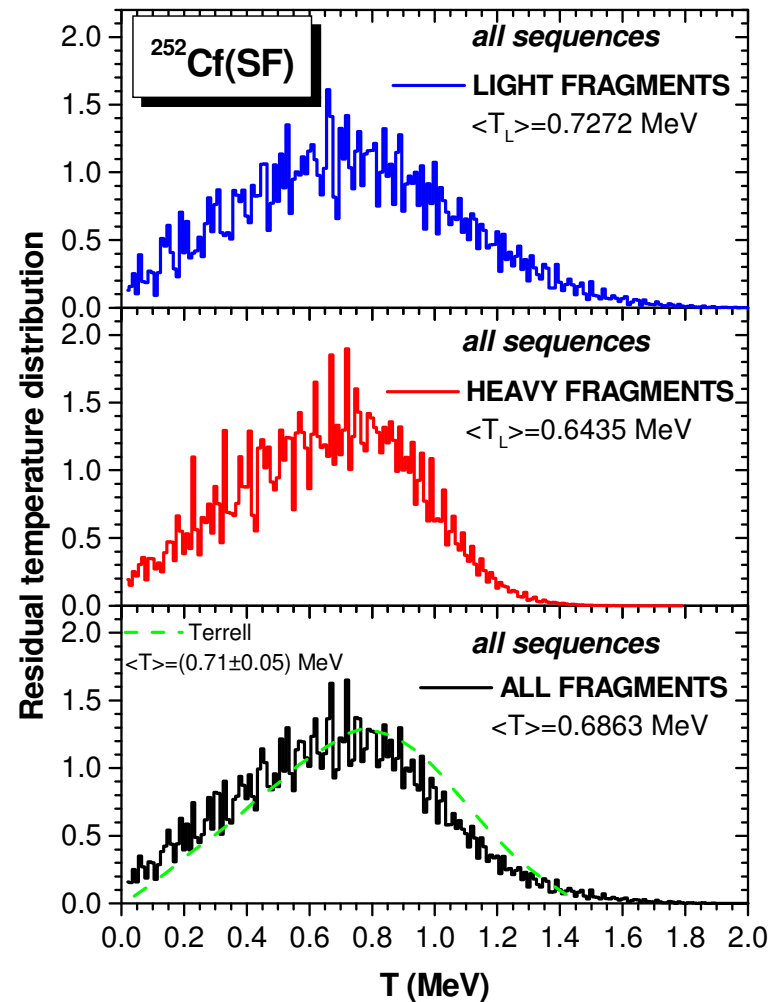


Examples of DSE results for residual quantities → distribution of residual temperature
 Exemplified for $Y(A,TKE)$ VESPA and TXE partition based on modeling at scission

$P_k(T)$ for each emission sequence



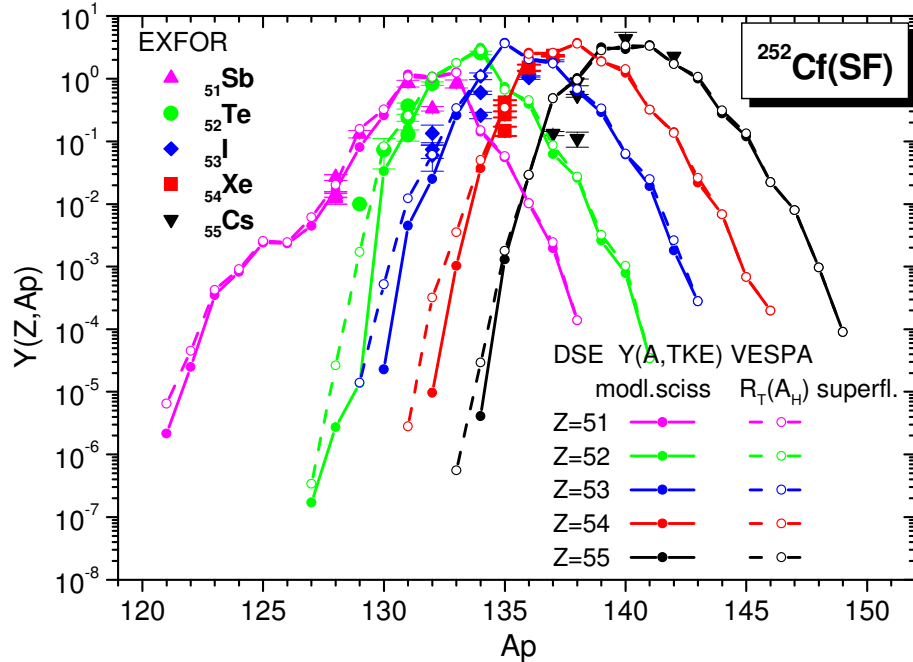
$P_{L,H}(T)$, $P(T)$ for all emission sequences



These distributions can be well approximated by triangular shapes,
 Such triangular $P(T)$ are used in prompt emission models with a global treatment of sequential emission (e.g. PbP, LAM)

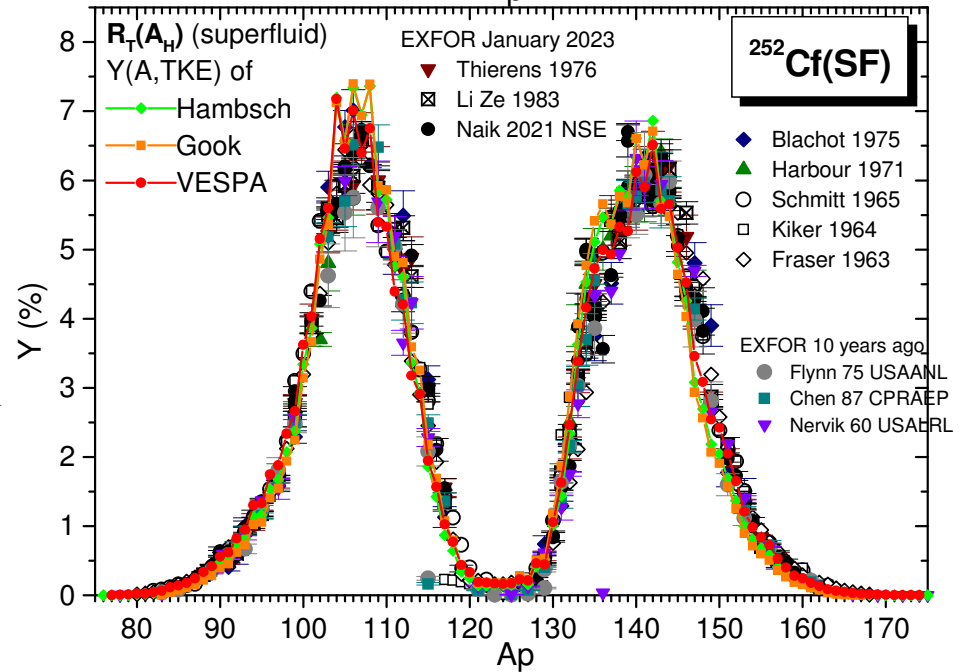
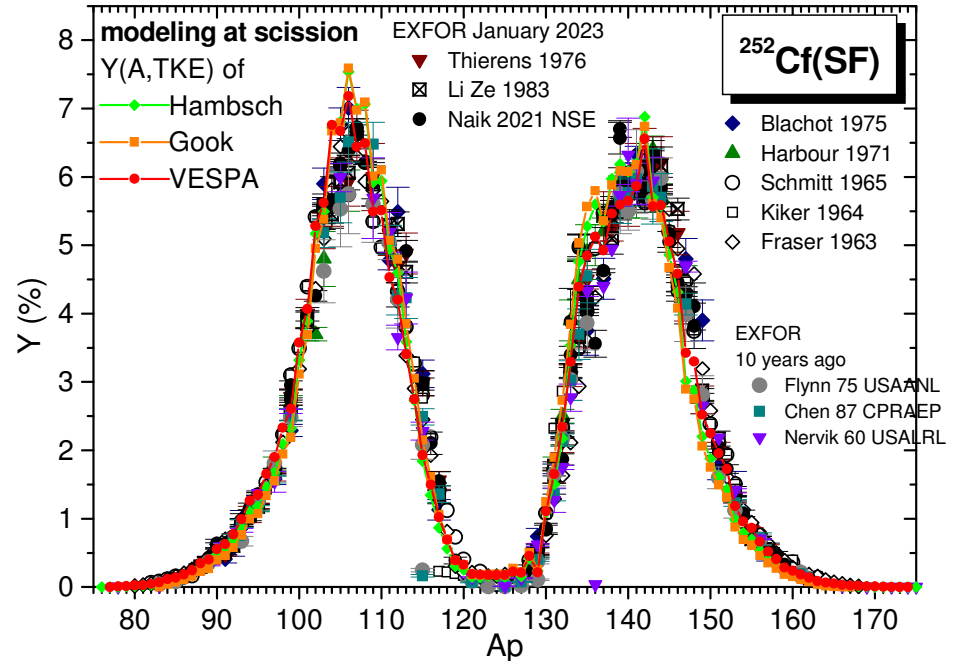
Independent FPY: DSE results with two energy partitions and three Y(A,TKE) data

In the DSE model:
 for each initial configuration (A,Z,TKE) appearing with the probability Y(A,Z,TKE) the mass number of the last residual fragment is well determined as $A_p = A - n$ (in which n is the number of emission sequences (or prompt neutrons))



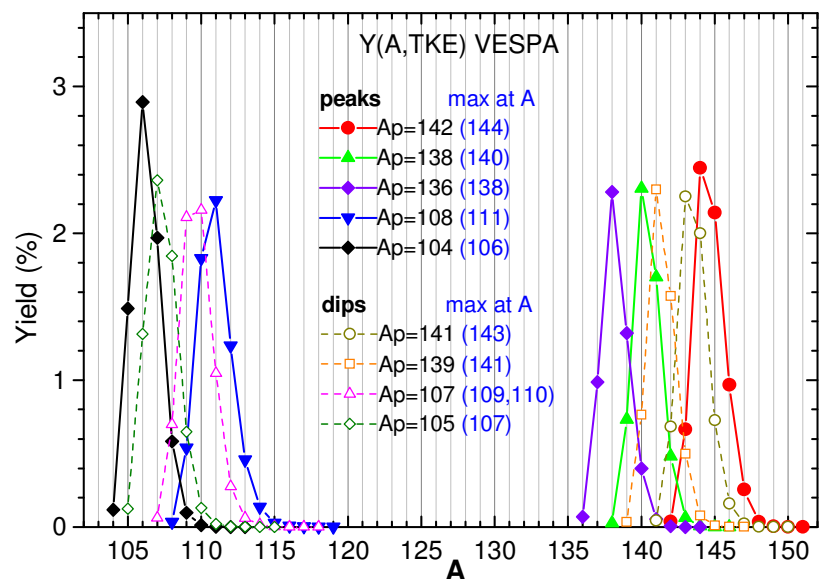
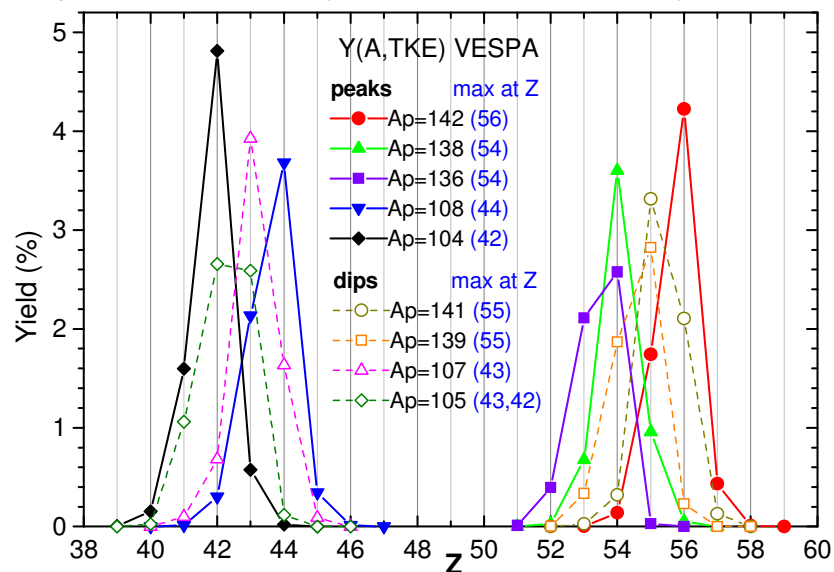
Differences in the $Y(A_p)$ structure due to both the Y(A,TKE) distribution and the TXE partition are seen →

Pronounced peaks and dips are seen in the $Y(A_p)$ structure: e.g. peaks at $A_p = 142, 138, 136, 104, 108$ and dips at $A_p = 141, 139, 107, 105$

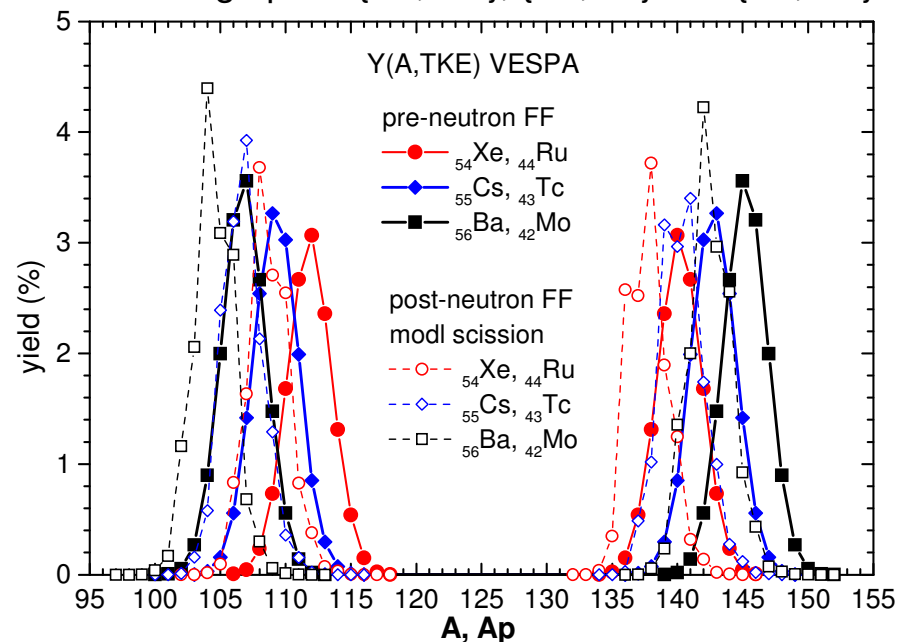


Identification of pre-neutron fragments which lead to pronounced peaks and dips in the $Y(A_p)$ structure

Charge and mass distributions of pre-neutron fragments leading to the mass numbers A_p of post-neutron fragments indicated in figures



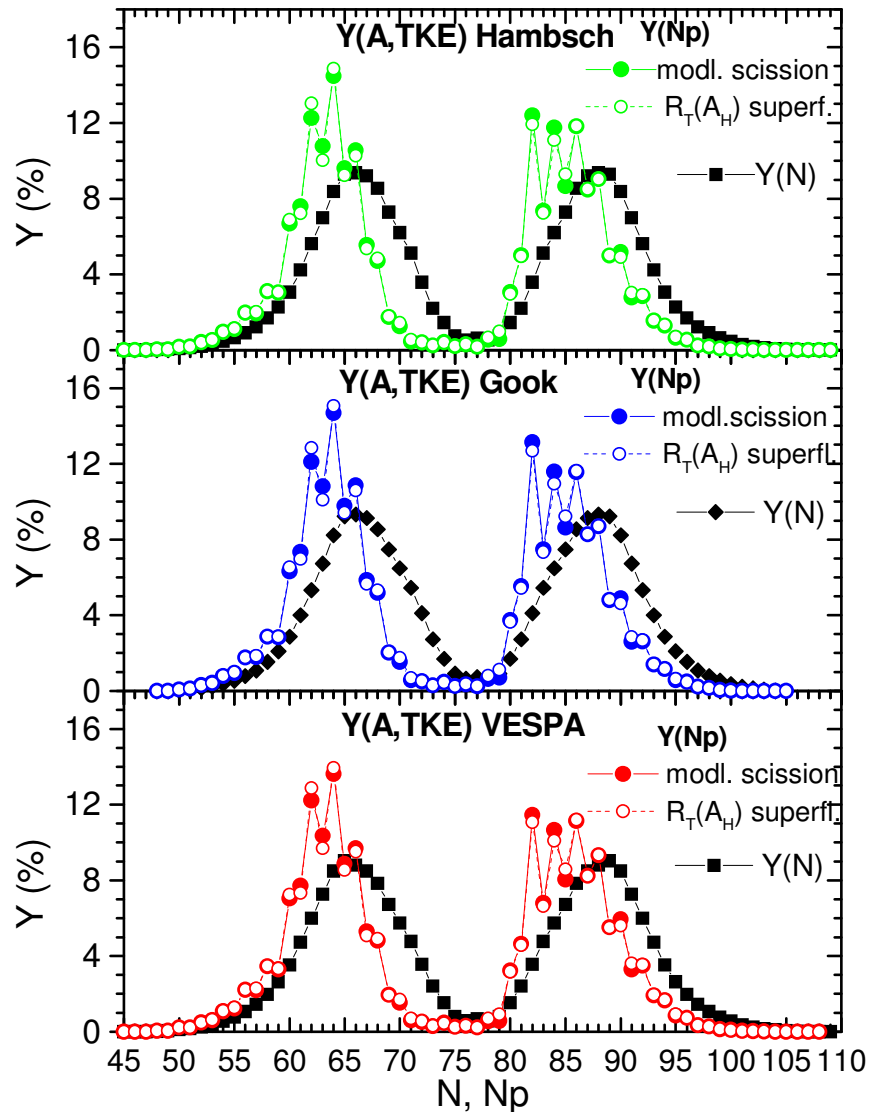
Pre-neutron fragment yields $Y(Z,A)$ (full symbols) and post-neutron fragment yields $Y(Z,A_p)$ (open symbols) of the charge pairs {Ba, Mo}, {Cs, Tc} and {Xe, Ru}.



Pronounced **peaks** in the $Y(A_p)$ structure at $A_p = 142, 138, 108, 104$ are due to the high maxims of post-neutron fragment yields of ^{56}Ba , ^{54}Xe , ^{44}Ru and ^{42}Mo , respectively (**even Z**). The post-neutron fragment yields of ^{55}Cs and ^{43}Tc (**odd-Z**) contribute to the **dips** at $A_p = 141, 139$ and 107 , respectively.

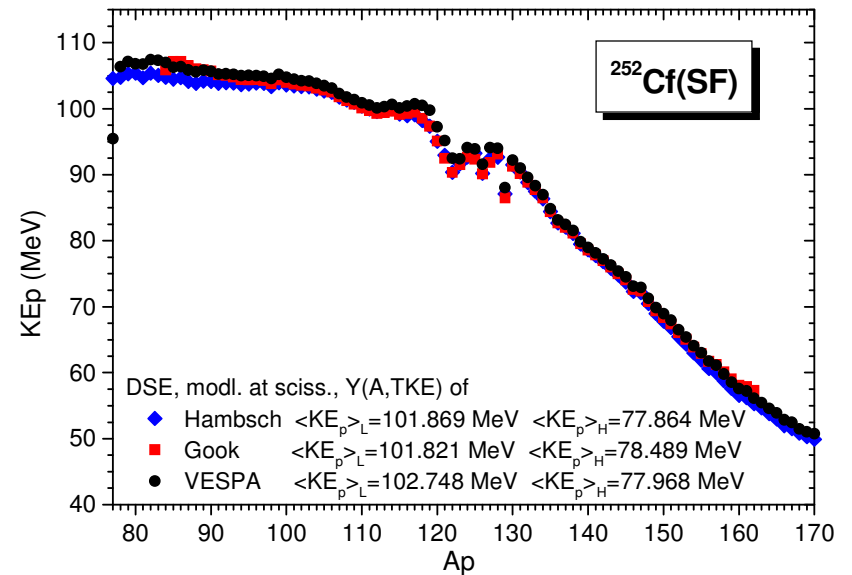
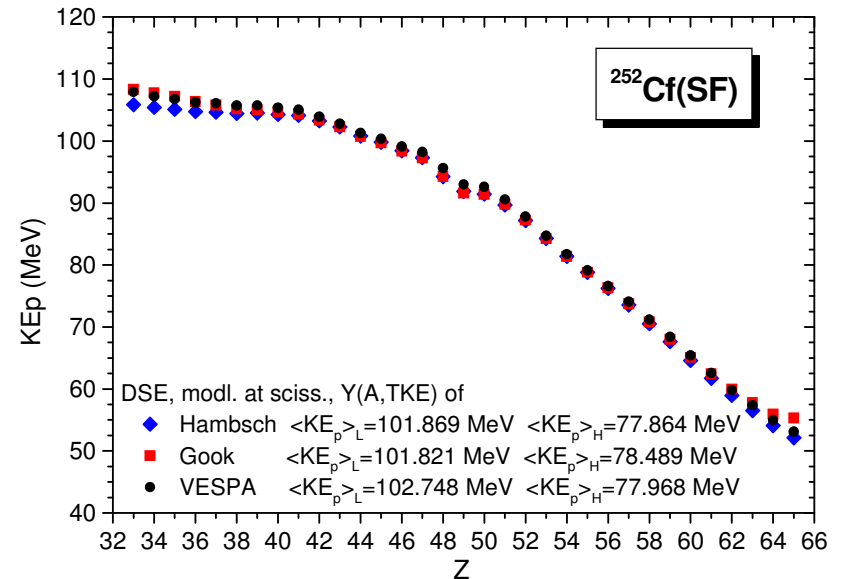
The even-odd effect in fragment charge plays a role in the case of $^{252}\text{Cf}(\text{SF})$, too. But it is less pronounced than in the case of $^{235}\text{U}(n_{\text{th}},\text{f})$ because the global e-o effect in $Y(Z)$ is 10 times lower in the case of $^{252}\text{Cf}(\text{SF})$ compared to $^{235}\text{U}(n_{\text{th}},\text{f})$.

Isotonic yields of pre- and post-neutron fragments: $Y(N)$, $Y(N_p)$

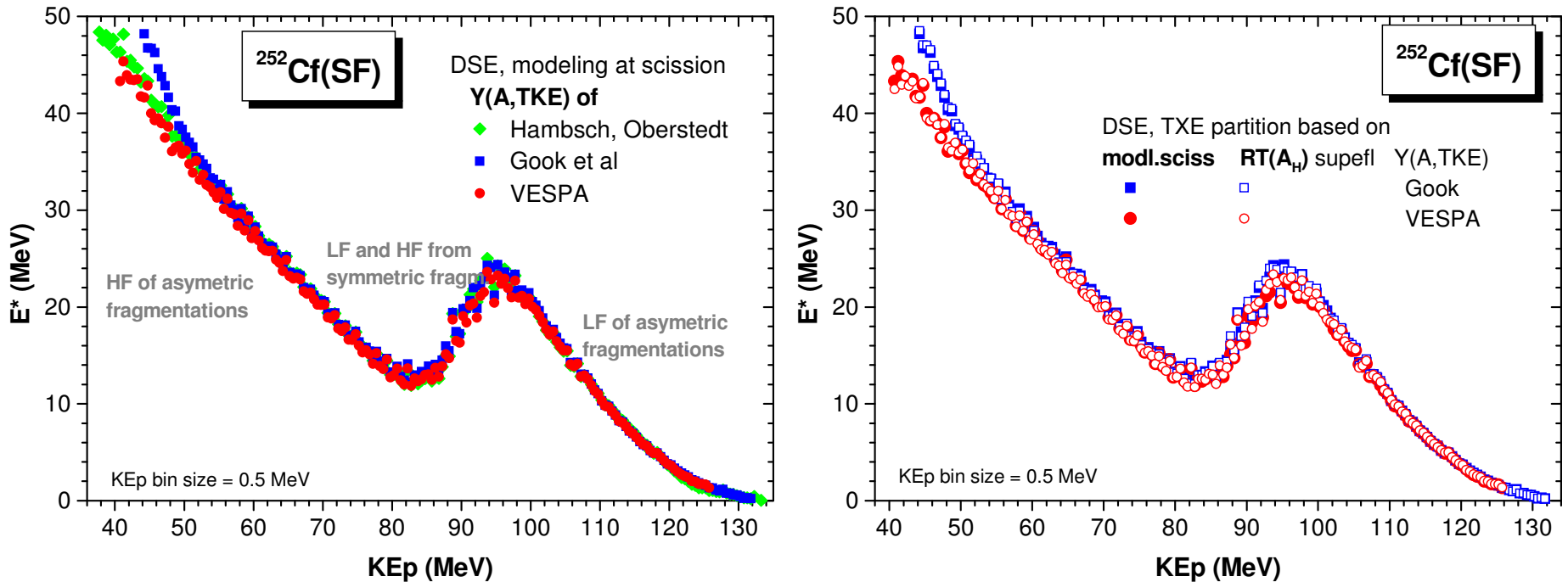


Pronounced peaks at $N_p=82$ (magic), 84, 86, 64, 62 (corresponding to peaks in the $Y(A_p)$ structure at $A_p = 138, 140, 142, 108, 106, 104$) are due to even- Z fragments $_{56}\text{Ba}$, $_{54}\text{Xe}$, $_{44}\text{Ru}$, $_{42}\text{Mo}$ coming from very probable pre-neutron fragmentations

Kinetic energies distributions of post-neutron fragments $KE_p(Z)$, $KE_p(A_p)$



Correlation between the excitation energy E^* of fully accelerated pre-neutron fragments and the kinetic energy KE_p of post-neutron fragments



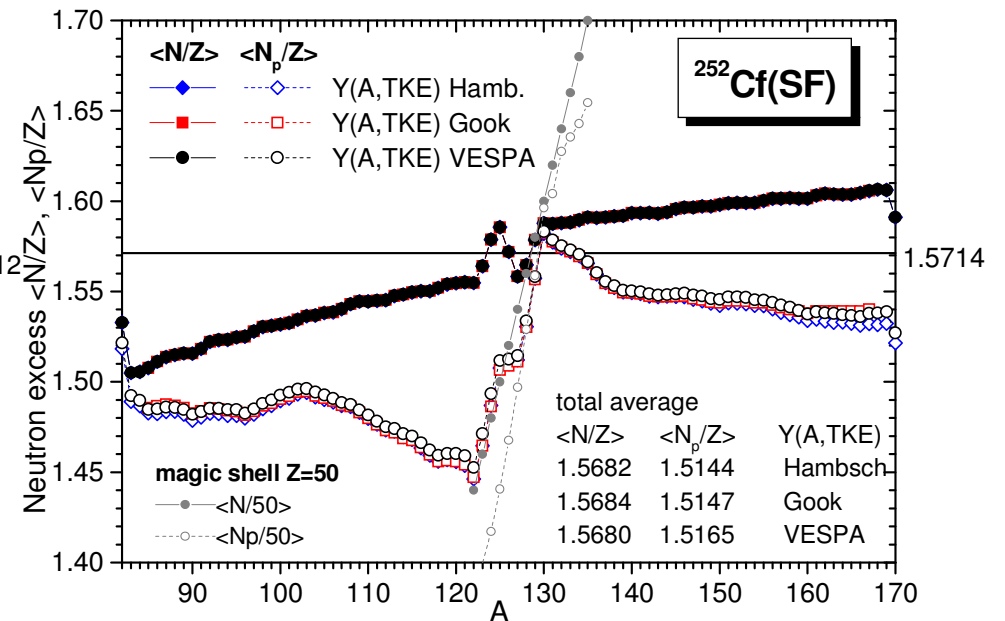
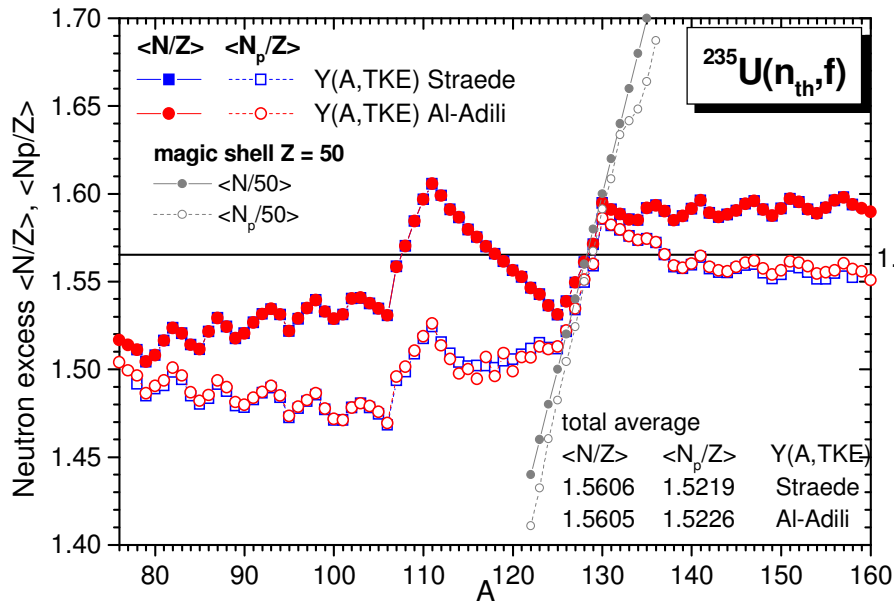
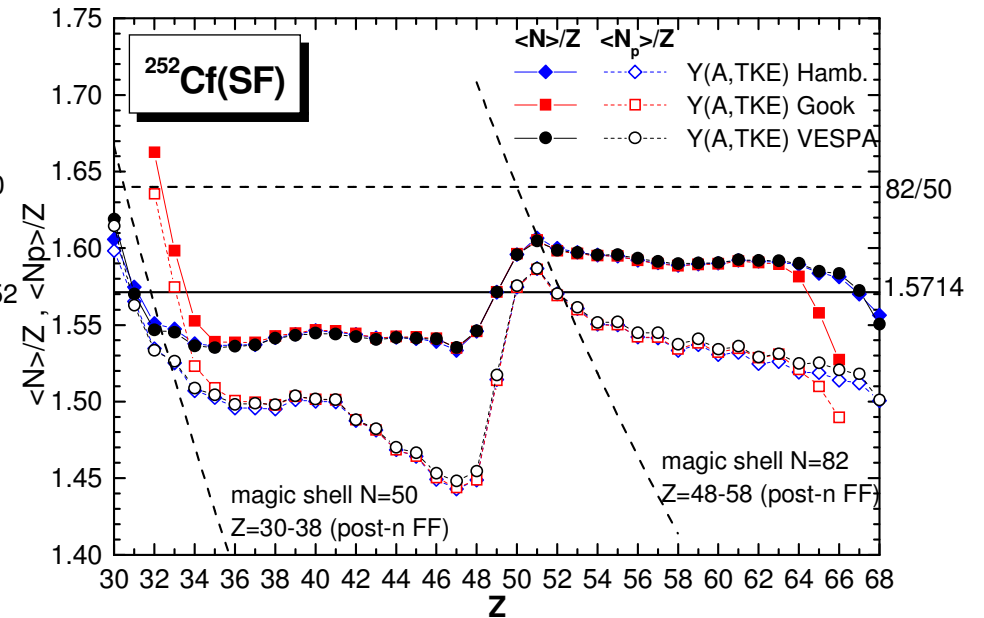
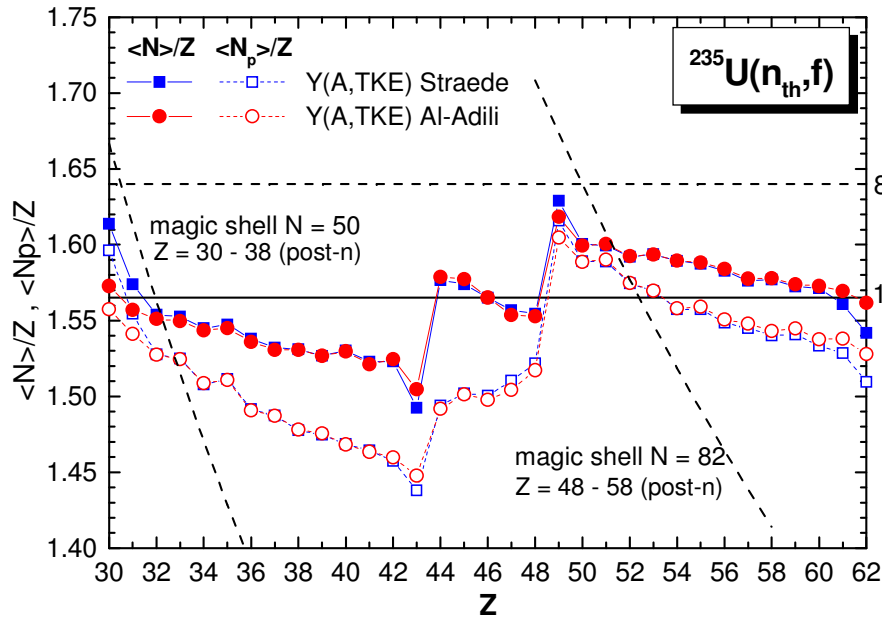
$E^*(KE_p)$ exhibits a well delineated sawtooth shape. It looks as a reflection in mirror of the sawtooth shape of $v(A)$ and $E^*(A)$

This sawtooth shape of $E^*(KE_p)$ consists of two almost linear decreasing parts which correspond to the light and heavy fragments, respectively, coming from asymmetric fragmentations. They are linked by an increasing part which corresponds to both light and heavy fragments from near symmetric fragmentations.

In the case of $^{252}\text{Cf}(\text{SF})$ the increasing part is located at KE_p between of about 85 and 95 MeV, while in the previous investigated case of $^{235}\text{U}(n_{\text{th}},f)$ this increase takes place at KE_p from about 80 to 90 MeV.

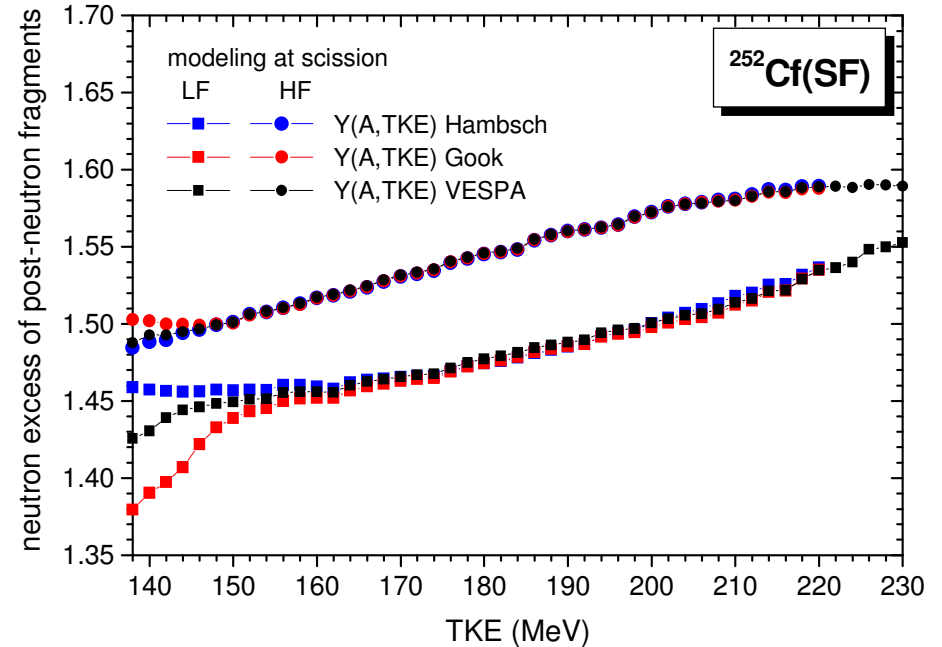
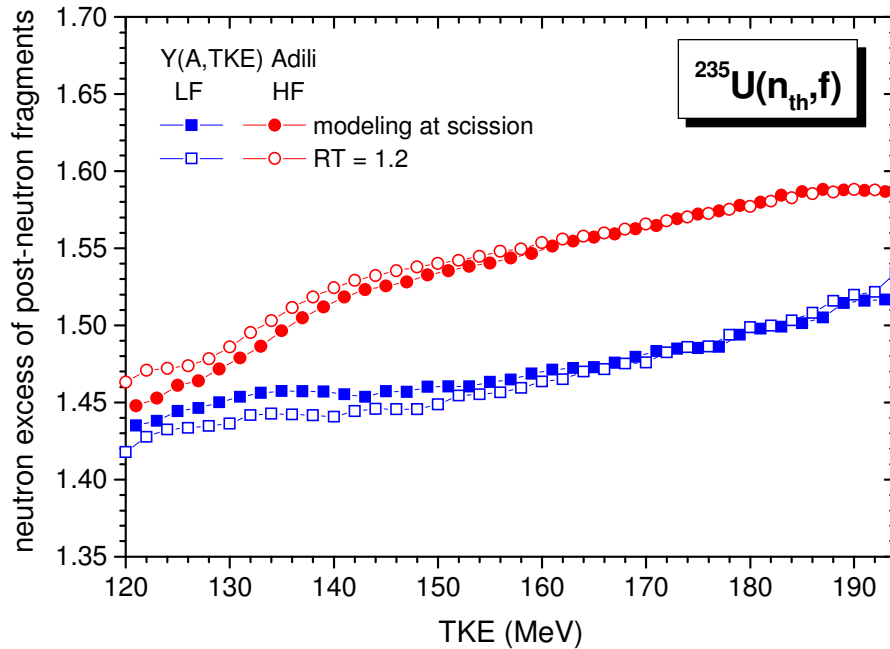
Neutron excess of pre- and post-neutron fragments (N/Z , N_p/Z)

$\langle N/Z \rangle$ and $\langle N_p/Z \rangle$ obtained by averaging N/Z and N_p/Z of (A,Z,TKE) configurations over $Y(A,Z,TKE)$



Neutron excess of post-neutron fragments as a function of TKE

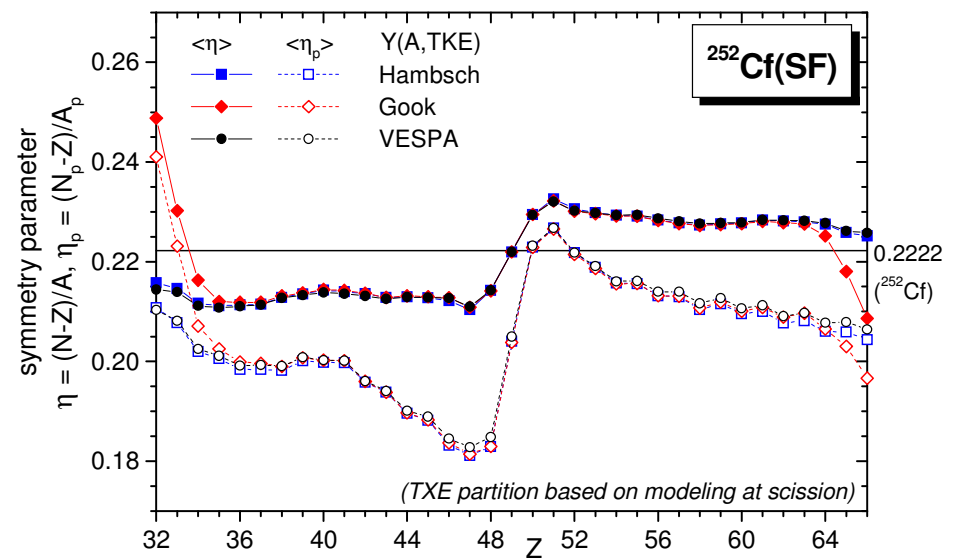
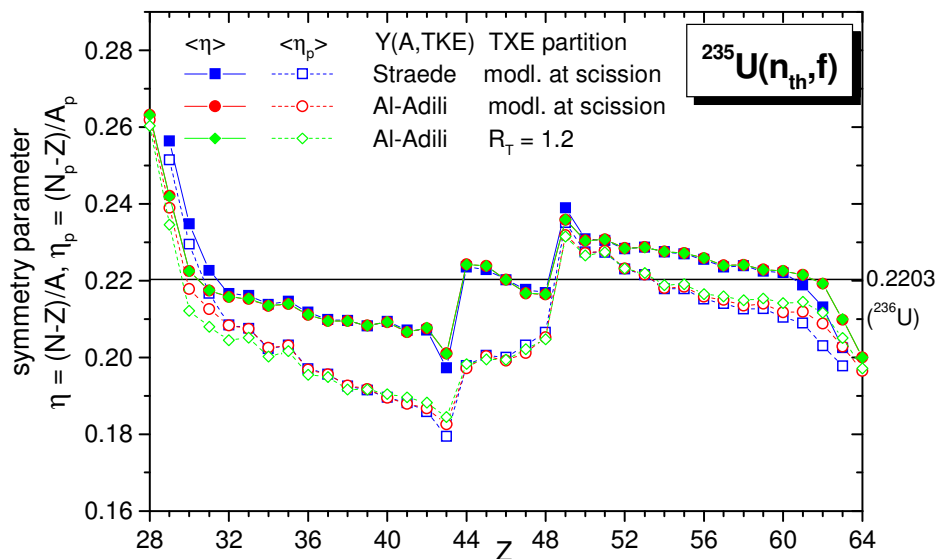
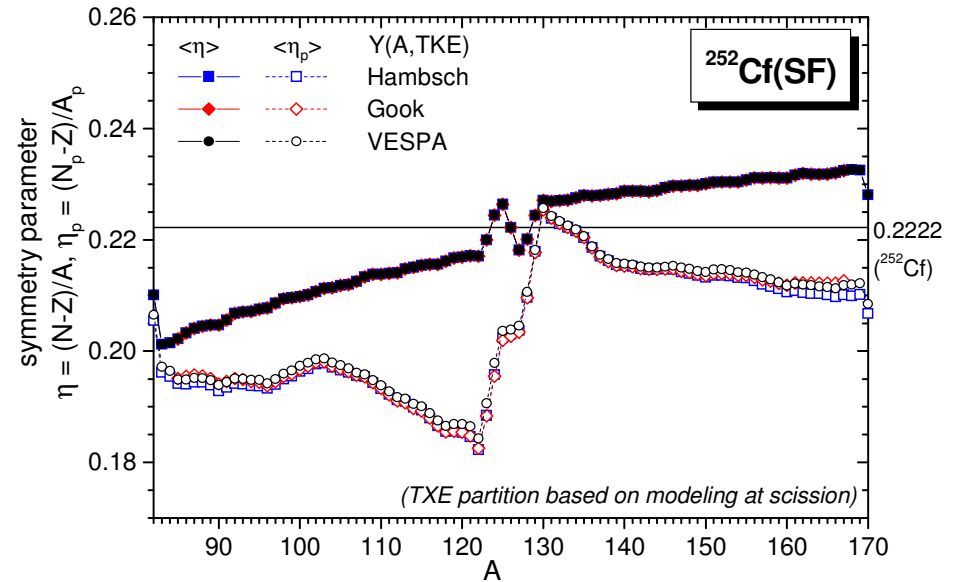
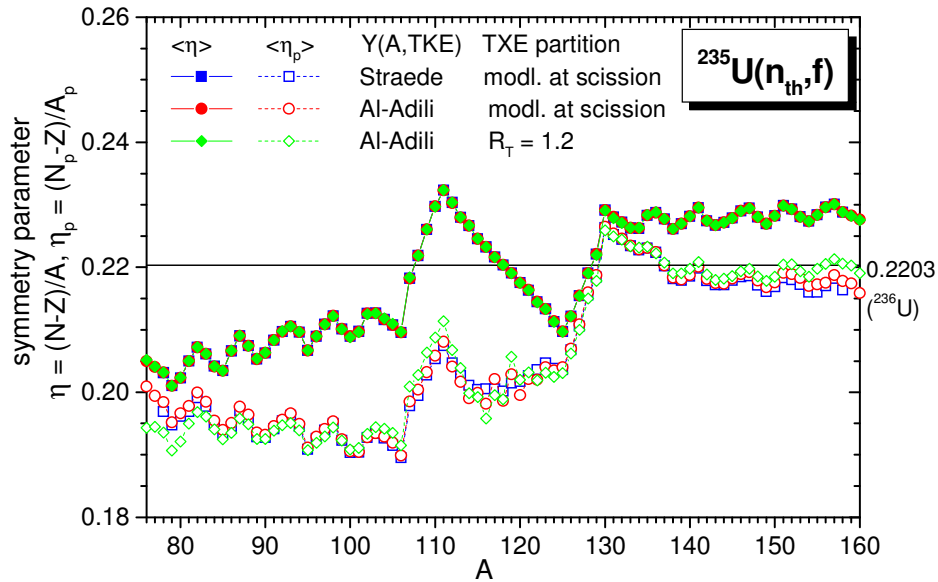
The average neutron excess of post neutron fragments as a function of TKE is obtained by averaging the neutron excesses of post-neutron fragments corresponding to the (A,Z,TKE) configurations over the $Y(A,Z,TKE)$ distribution, by summing over A and Z separately for the light and heavy fragment groups.



The average neutron excess of the heavy post-neutron fragments is higher than the neutron excess of the light ones. A visible increase of the average neutron excess of post-neutron fragments with increasing of TKE is seen. This behaviour is explained by the fact that higher TKE values lead to lower TXE values, which mean lower excitation energies (E^*) of fully accelerated pre-neutron fragments, which are reflected in less emitted prompt neutrons, proved by the linear decrease of $\langle v \rangle(TKE)$. In other words a great part of these pre-neutron fragments with low E^* (corresponding to high TKE) do not emit prompt neutrons and these fragments, having higher neutron excesses, contribute to the higher average values of the neutron excess at higher TKE values.

Symmetry parameter of pre- and post-neutron fragments ($\eta = (N-Z)/A$, $\eta_p = (N_p-Z)/A_p$)

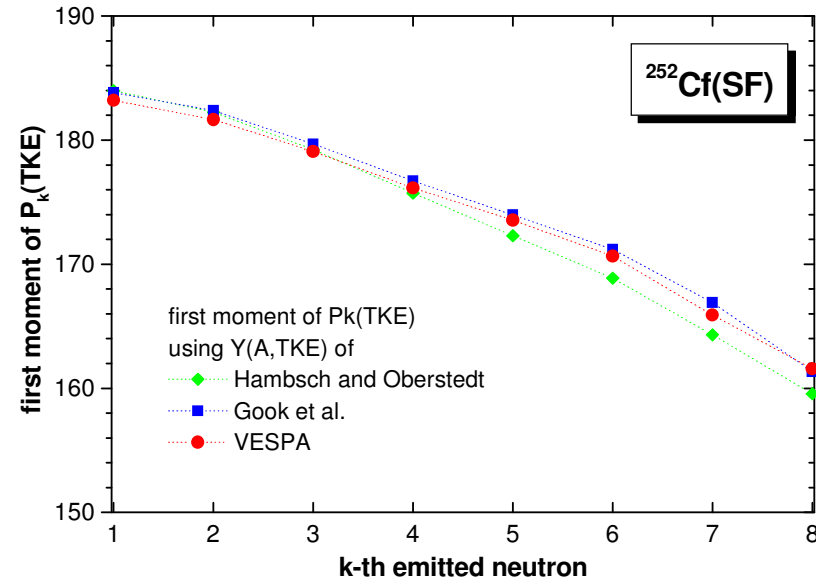
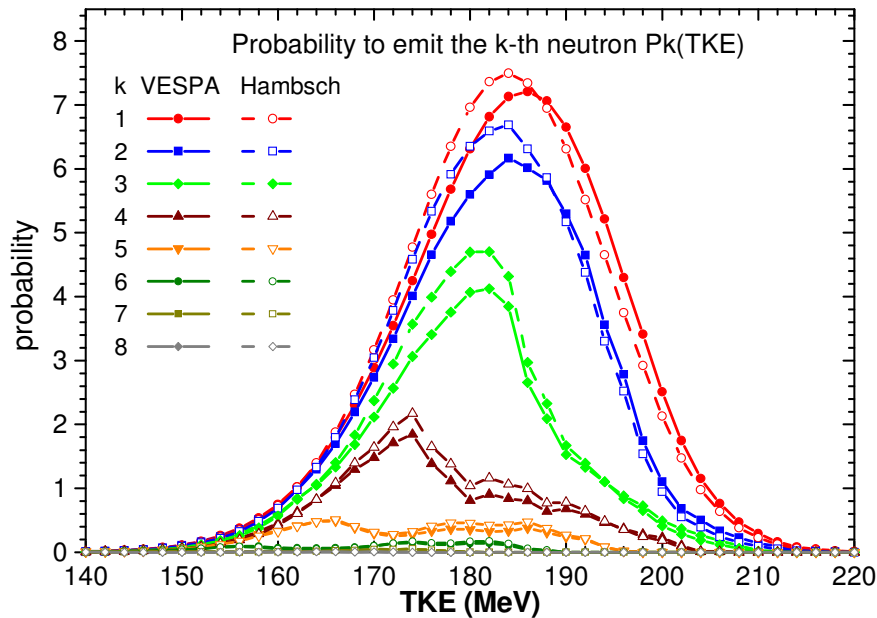
$\langle \eta \rangle$ and $\langle \eta_p \rangle$ as a function of A or of Z are obtained by averaging η and η_p corresponding to the (A,Z,TKE) configurations over Y(A,Z,TKE)



Influence of $Y(A, TKE)$ on the probability to emit each prompt neutron Pn_k

Note: Pn_k is the probability to emit each prompt neutron, i.e. the first one $k=1$, the second one $k=2$, etc. It **must not be confused** with the distribution of prompt neutron multiplicity $P(v)$ which means the probability to emit one neutron ($v=1$), two neutrons ($v=2$), three neutrons ($v=3$) etc.

as a function of TKE: $Pn_k(TKE)$



The hump heights are decreasing when k is increasing, this is obvious because **the first and second neutrons are emitted by the majority of $\{A, Z, TKE\}$ configurations while the third neutron, the 4-th neutron etc. can be emitted by less and less initial configurations.**

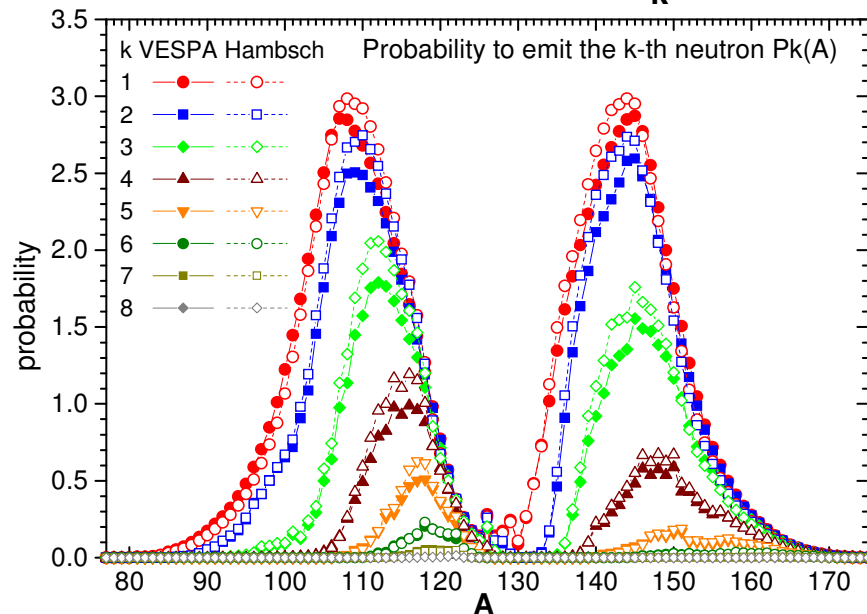
It can be observed that the maximums of $Pn_k(TKE)$ are placed at lower TKE values when k is increasing (i.e. the shift to left of $Pn_k(TKE)$ with increasing k). This can be easily explained by the obvious fact that **lower TKE values lead to higher TXE values which make possible the emission of more prompt neutrons.**

This is proved by the first moments of $Pn_k(TKE)$ (see the right frame)

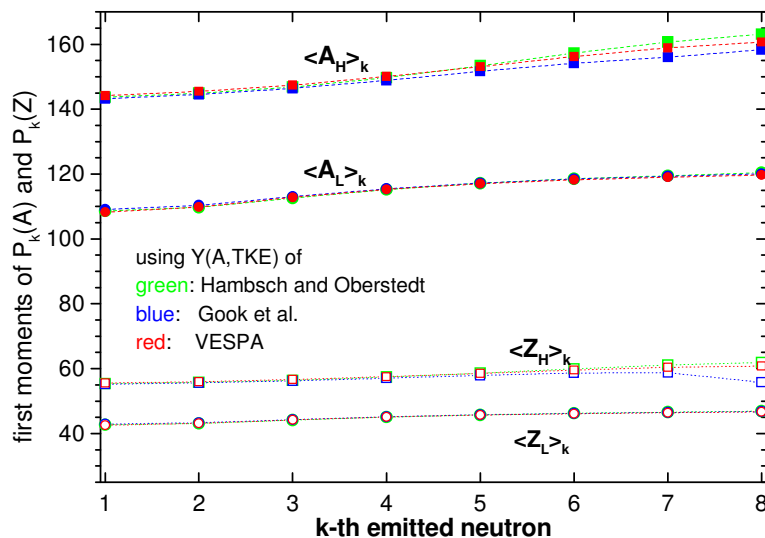
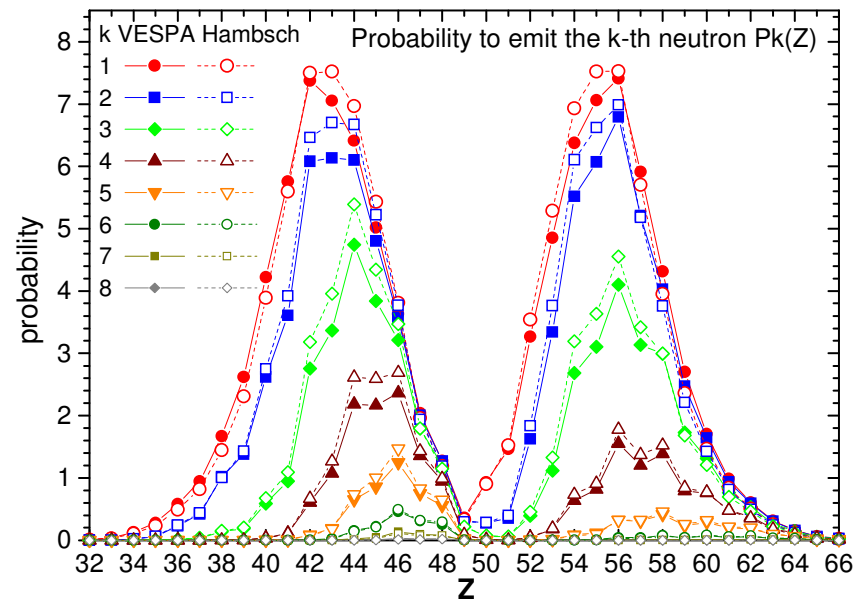
Influence of $Y(A, TKE)$ on the probability to emit each prompt neutron Pn_k

continuation

as a function of A: $Pn_k(A)$



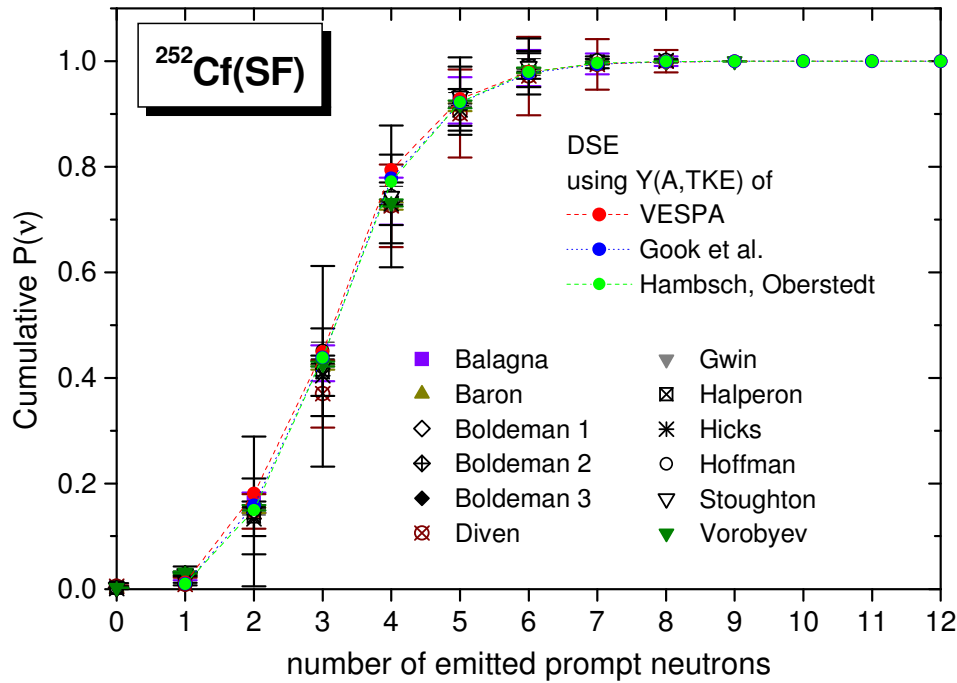
as a function of Z: $Pn_k(Z)$



The hump heights are decreasing when k is increasing. This is obvious because the first neutron and the second neutron are emitted by the majority of initial fragments, while the next neutrons (the third, 4-th, 5-th etc.) can be emitted by less and less initial fragments.

It can be observed that for the first and second emitted neutron i.e. $k = 1$ and $k = 2$, the humps corresponding to LF and HF groups are almost equal, while for higher k (i.e. the third, 4-th, 5-th... emitted neutron) the hump of LF is higher than the hump of HF, this proving again the general observation that the light fragment group emits more neutrons than the heavy fragment group.

Cumulative distribution of prompt neutron multiplicity



$$S(\nu) = \sum_{\nu=0}^{\nu} P(\nu)$$

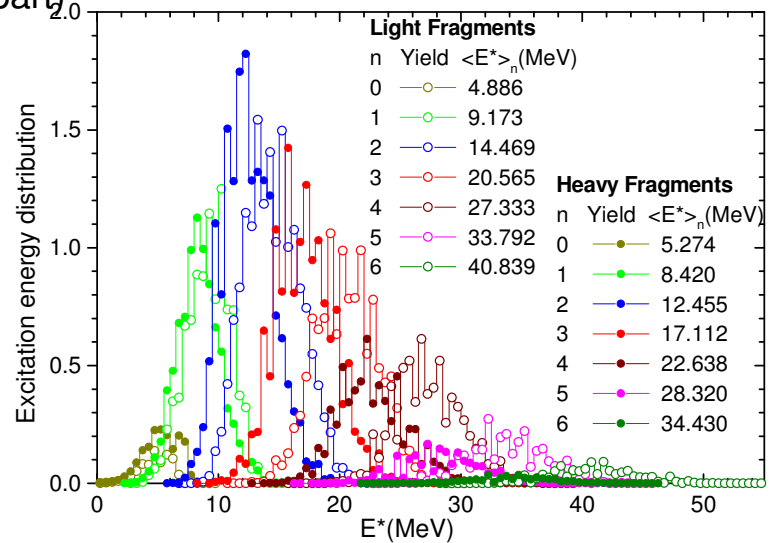
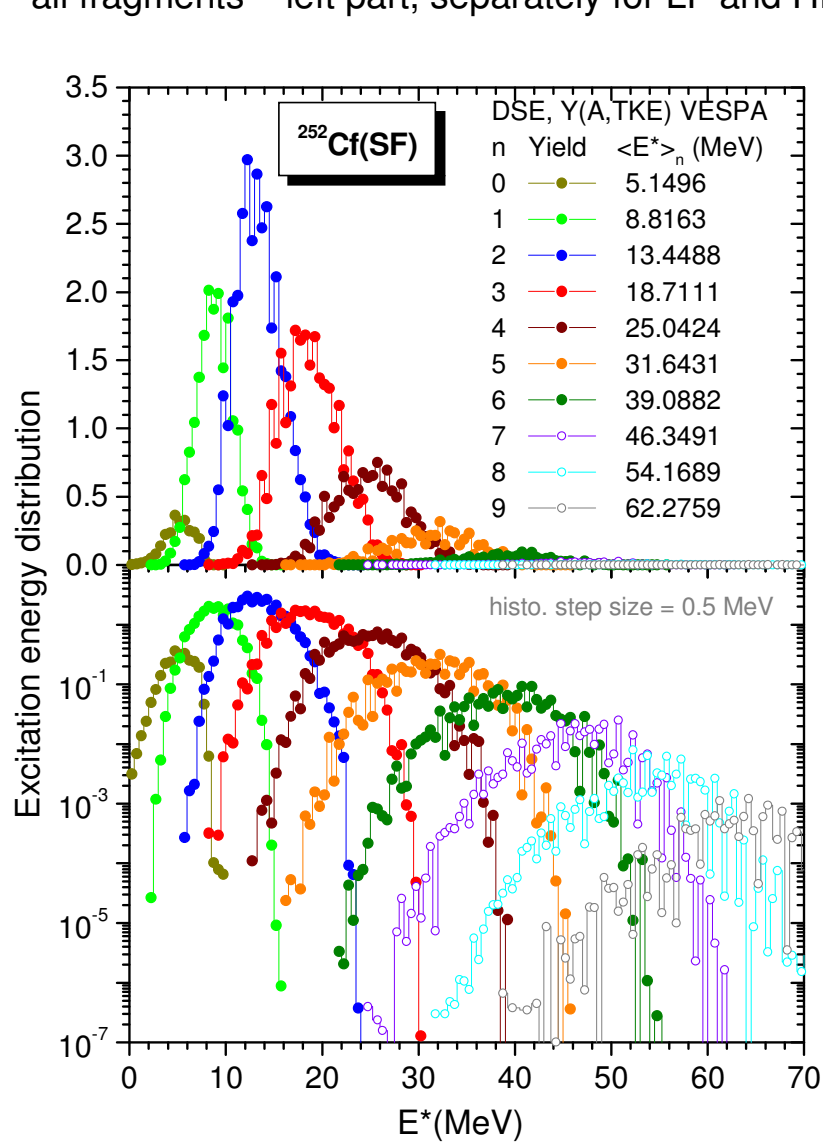
$P(\nu)$: the distribution of prompt neutron multiplicity

$$\langle \nu \rangle = \frac{\sum_{\nu=0}^{\nu \max} \nu P(\nu)}{\sum_{\nu=0}^{\nu \max} P(\nu)}$$

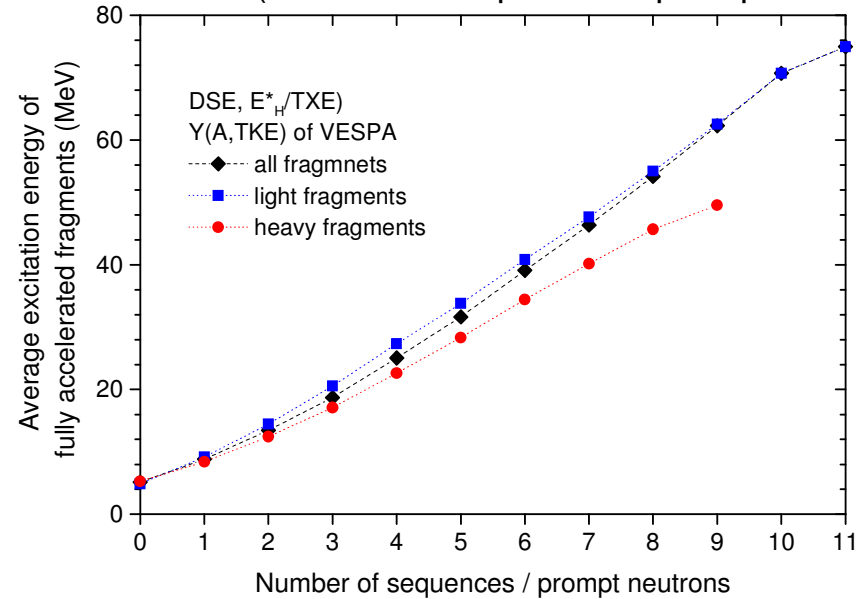
$P(\nu)$	$\langle \nu \rangle$	$P(\nu)$	$\langle \nu \rangle$
Exp. Balagna	3.738 ± 0.215	Exp. Halperin	3.7580 ± 0.3359
Exp. Baron	3.783 ± 0.034	Exp. Hicks	3.8234 ± 0.2137
Exp. Boldeman 1	3.757 ± 0.015	Exp. Hoffman	3.7198 ± 0.7042
Exp. Boldeman 2	3.7566 ± 0.0147	Exp. Vorobyev	3.756 ± 0.038
Exp. Boldeman 3	3.7571 ± 0.0182	DSE, VESPA	3.6870
Exp. Diven	3.876 ± 0.424	DSE, Gök	3.7489
Exp. Gwin	3.7733 ± 0.0120	DSE, Hamsch	3.7582

Distributions of the excitation energies of pre-neutron fragments $Y_n(E^*)$ leading to each number 'n' of emission sequences (n = 1, 2, 3...)

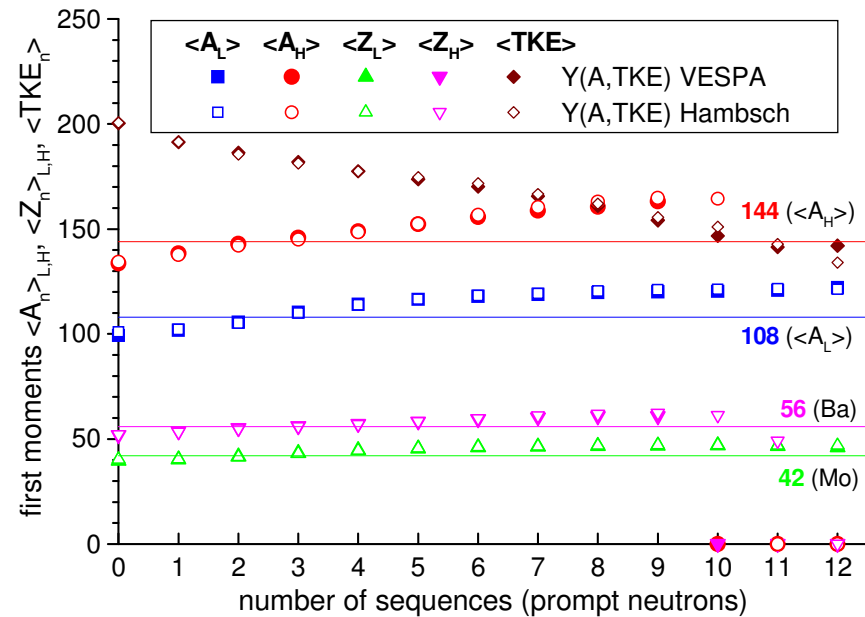
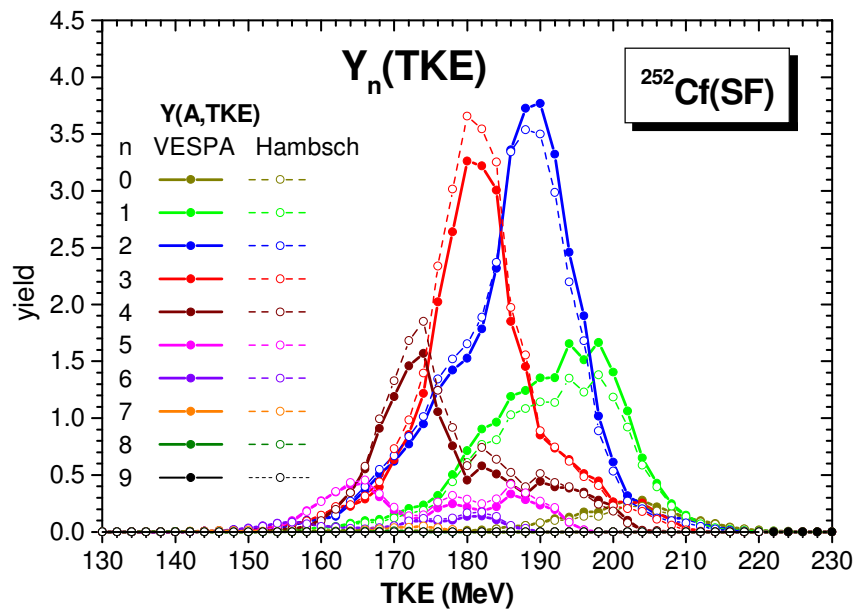
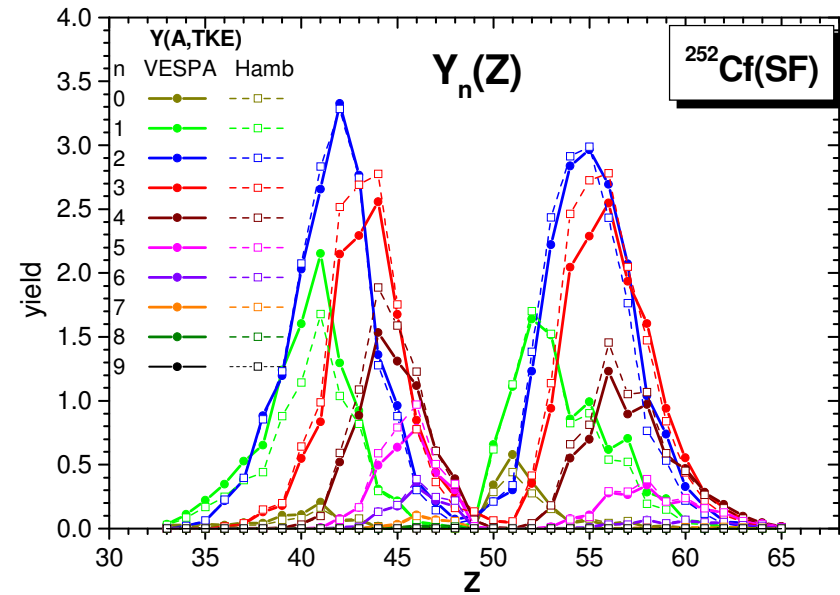
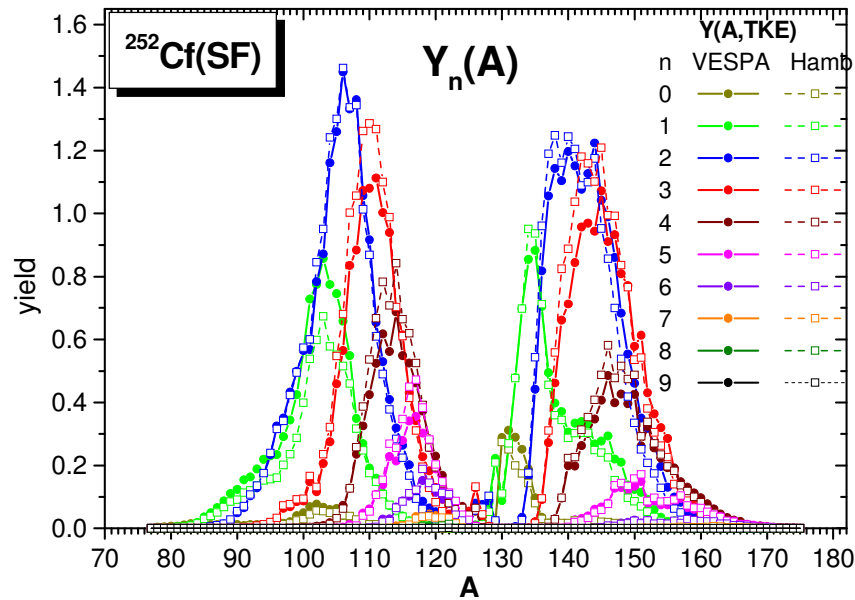
all fragments – left part, separately for LF and HF – right part)



First moments of $Y_n(E^*)$ ($\langle E^*_{L,H} \rangle_n$, $\langle E^* \rangle_n$) as a function of n (number of sequences / prompt neutr.)



Distributions of mass, charge and TKE of pre-neutron fragments leading to each number 'n' of emission sequences (n = 1, 2, 3...)



Conclusions

Validation of prompt emission results of DSE by their good description of experimental data.

The results of independent FPY ($Y(Z, A_p)$, $Y(A_p)$) are obtained in good agreement with the experimental data

- In the case of $^{252}\text{Cf}(\text{SF})$ the influence of TXE partition on the $Y(A_p)$ structure is lower than in the previous studied case of $^{235}\text{U}(n_{\text{th}}, \text{f})$ because this time R_T is taken as a function of A_H by a parameterization which approximates well the shape of $R_T(A_H)$ obtained from modeling at scission.
- The influence of the $Y(A, \text{TKE})$ distribution on independent FPY is more pronounced than in the case of $^{235}\text{U}(n_{\text{th}}, \text{f})$, leading to differences not only in the magnitude of visible peaks and dips in $Y(A_p)$ but also in their position.
- Again the pronounced peaks in the $Y(A_p)$ structure are due to even-Z fragments and the pronounced dips to odd-Z fragments but the role of the even-odd effect in fragment charge is less important than in the previous studied case because the global even-odd effect in $Y(Z)$ is almost 10 times lower in the case of $^{252}\text{Cf}(\text{SF})$ compared to $^{235}\text{U}(n_{\text{th}}, \text{f})$.
 - The correlation between E^* and KE_p is maintained in the case of $^{252}\text{Cf}(\text{SF})$, too. It consists of a well delineated sawtooth shape which looks as a reflection in mirror of the well-known sawtooth shape of $v(A)$ and $E^*(A)$
 - The large number of (A, Z, TKE) configurations taken into account in DSE calculations allows to investigate the neutron excess of pre- and post-n FF of both $^{235}\text{U}(n_{\text{th}}, \text{f})$ and $^{252}\text{Cf}(\text{SF})$, revealing interesting features, e.g.: both neutron excesses $\langle N/Z \rangle(A)$, $\langle N_p/Z \rangle(A)$ (and also the symmetry parameters $\langle \eta \rangle(A)$, $\langle \eta_p \rangle(A)$) exhibit oscillations with a periodicity of about 5 u (pronounced for $^{235}\text{U}(n_{\text{th}}, \text{f})$, less visible for $^{252}\text{Cf}(\text{SF})$). They are due to $\Delta Z(A)$ which exhibits similar oscillations. The magnitude of the global e-o effect is reflected in the magnitude of oscillation amplitudes in $\Delta Z(A)$ and as consequence in the magnitude of oscillation amplitudes of $\langle N/Z \rangle(A)$ and $\langle N_p/Z \rangle(A)$. The almost linear increase of neutron excess $\langle N_p/Z \rangle(\text{TKE})$ is explained, too.
 - The E^* distributions of pre-neutron fragments leading to each number 'n' of emission sequences /prompt neutrons $Y_n(E^*)$ show a correlation expressed by the linear increase of the first moments $\langle E^*_n \rangle_{L,H}$ of these distributions with increasing number of sequences (the increasing slope of $\langle E^*_n \rangle$ of LF is visibly higher than that of HF)
 - The highest pre-neutron fragment distributions $Y_n(A)$, $Y_n(Z)$ are those for $n = 2, 3, 4$, confirming again the values of $\langle v \rangle$ between 3.7 and 3.8, on which the experimental $P(v)$ is centered. $Y_n(A)$ and $Y_n(Z)$ of light fragment group are higher than those of heavy fragment group, confirming the usual statement that the LF emit more neutrons than the HF. The first moments $\langle Z_n \rangle_{L,H}$ as a function of n (number of sequences) are almost constant with values of about 56 (Ba) and 42 (Mo), which correspond to the most probable charge fragmentation.

Outlook

Such studies will be extended to other thermal neutron induced fissions, e.g. $^{239}\text{Pu}(n_{\text{th}},f)$, $^{233}\text{U}(n_{\text{th}},f)$ and to the fast neutron induced fission, e.g. $^{234}\text{U}(n,f)$, $^{237}\text{Np}(n,f)$ in order to investigate different aspects, such as:

- The influence of TXE partition and of $Y(A,\text{TKE})$ data on independent FPY and other quantities characterizing the post-neutron fragments
- The correlation between the magnitude of the even-odd effect in the fragment charge distribution and the magnitude and position of pronounced peaks and dips in the structure of post-neutron fragment yields $Y(A_p)$, $Y(N_p)$
- Behaviours of neutron excess (N/Z) and symmetry parameter ($\eta=(N-Z)/A$) of pre- and post-neutron fragments (as a function of Z , of A , of TKE) and their correlation with the magnitude of the even-odd effect in fragment charge
- The correlation between E^* (of pre-neutron FF) and KE_p (of post-neutron FF), to see if this correlation is maintained in the case of other fissioning nuclei, which differences appear etc.
- Possible correlations related to the distributions $Y_n(E^*)$, $Y_n(A)$, $Y_n(Z)$, $Y_n(\text{TKE})$

Thanks for your attention !